Rate- and Depth-dependent Fracture Failure of Cartilage Using Microindentation Testing

Guebum Han[1], Corinne R. Henak[1,2], Melih Eriten[1]
[1]Department of Mechanical Engineering, [2]Department of Biomedical Engineering, University of Wisconsin, Madison, WI
ghan28@wisc.edu

Disclosures: Guebum Han (N), Corinne R. Henak (N), Melih Eriten (N)

INTRODUCTION: Articular cartilage has remarkable rate-dependent mechanical properties to support high loads and dissipate energy [1–3]; such characteristics originate from the combined effect of the solid matrix (collagen fibrils and proteoglycans) and interstitial fluid. Collagen fibrils primarily support instantaneous loads by resisting tension created when interstitial fluid is pressurized [1,3,4]. Proteoglycans mainly support compressive loads with mutually repulsive forces and osmotic pressure [2,5]. Fluid-solid frictional interaction (poroelasticity) and solid matrix intrinsic viscoelasticity are the two main energy dissipation mechanisms in cartilage [1,2,6,7]. While numerous studies have tested cartilage mechanics prior to failure as a function of rate and depth, few studies have evaluated cartilage fracture. Matrix cohesion is strongly governed by collagen fibrils [8], suggesting that fibrils play an important role in fracture behavior. The fracture toughness of articular surface with microindentation techniques was measured at a single loading rate [9]. Thus, the objective of this study was to determine rate- and depth-dependent crack nucleation.

METHODS: Eight full-thickness cartilage samples were harvested from four porcine patellae (5-6 months old) using a 6 mm diameter coring tool and scalpel. Subchondral bone was removed using a microtome. Each sample was cut into paired hemi-cylindrical samples, which were tested at the articular surface and deep zone (Fig. 1). Samples were attached to a Petri dish using cyanoacrylate (Super Bonder 495, Loctite).

Time-dependent cartilage fracture behavior was determined via microindentation tests at different loading rates (Fig. 1). Tests were conducted on a Hysitron TI 950 TriboIndenter with a 20 μm radius diamond spherical-conical tip. Loading rates of 1, 300, and 600 μm/s were applied to samples until a sudden drop in load indicated crack nucleation (Fig. 1b). Critical load, critical displacement, and total work at crack nucleation were determined from load-displacement curves. After fracture tests, samples were stained with India ink and cracks were visualized using an optical microscope (Olympus IX71, Olympus) (Fig. 2a).

Differences between groups were assessed with two-tailed, paired t-tests (significant at $p \leq 0.05$, trend at $0.05 < p \leq 0.10$).

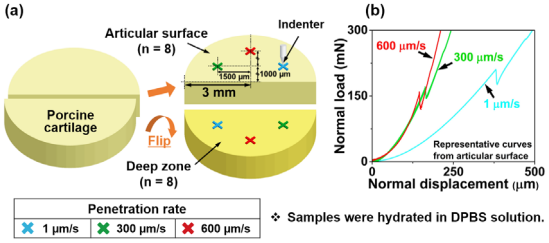

Fig. 1. (a) Schematic diagram of experimental setup and (b) representative curves showing sudden drops in load that correspond to crack initiation.

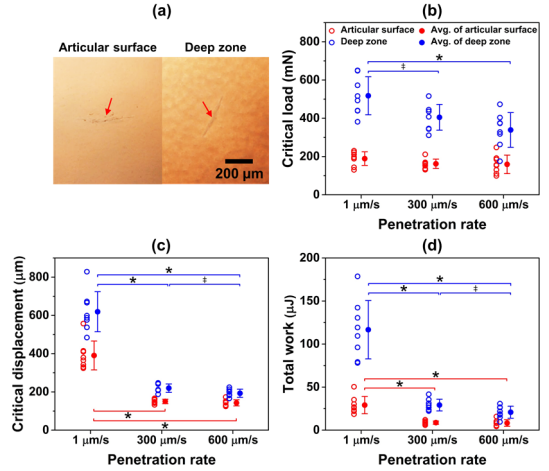

Fig. 2. (a) Representative optical images of cracks at 300 μm/s, (b) critical load, (c) critical displacement, and (d) total work. *=significant, ‡ =trend. Articular surface and deep zone were significantly different for all outputs at all rates and are not shown on the plots.

RESULTS: Critical load, critical displacement, and total work generally decreased with increasing rate (Fig. 2b-d). Critical loads for 1 μm/s were 1.53 times higher for deep zone than those for 600 μm/s ($p = 5.29\times10^{-3}$). Critical displacements for 1 μm/s were 2.74 times higher for articular surface ($p = 4.51\times10^{-5}$) and 3.21 times higher for deep zone ($p = 3.06\times10^{-6}$) than those for 600 μm/s. Total work for 1 μm/s was 3.49 times higher for articular surface ($p = 2.50\times10^{-4}$) and 5.60 times higher for deep zone ($p = 6.30\times10^{-5}$) than that for 600 μm/s. The parameter that was least affected by rate was the critical load, while total work was the most affected by rate.

Higher critical load, critical displacement, and total work were required to initiate a crack at the deep zone than at the articular surface (Fig. 2b-d). At 1 μm/s, critical load, critical displacement, and total work from deep zone were 2.74, 1.59, and 4.01 times higher than those from articular surface, respectively ($p < 3\times10^{-3}$). At 600 μm/s, critical load, critical displacement, and total work from deep zone were 2.13, 1.35, and 2.50 times higher than those from articular surface, respectively ($p < 7\times10^{-4}$). Differences between articular surface and deep zone were smaller at the high loading rate than at the low loading rate.

DISCUSSION: This study demonstrates that cartilage exhibits rate- and depth-dependent fracture behavior. Rate dependence can be interpreted based on cartilage poroelasticity and intrinsic viscoelasticity. Poroelastic energy dissipation is governed by the relaxation time constant, τ_{PE}. At 5 μm indentation, τ_{PE} = 1.92 seconds using linear poroelasticity and published material constants ($\tau_{PE} = a^2/(Hk)$, a: contact radius, H: aggregate modulus, and k: permeability [1,10,11]). While τ_{PE} increases with increased normal displacement, accurate estimates of the changes in material constants and the limits of linear poroelasticity preclude estimating τ_{PE} for larger displacements. Previous studies suggest that there are multiple relaxation time constants for cartilage intrinsic viscoelasticity: short $\tau_{1,VE} \approx 5$ milliseconds, intermediate $\tau_{2,VE} \approx 10$ seconds, and long $\tau_{3,VE} \approx$ 100-500 seconds [12–14].

At 600 μm/s, it is likely that most of the total work was used to create a fracture surface, with only a small amount of energy dissipated by intrinsic viscoelasticity. Crack nucleation occurred at 0.24±0.03 seconds for articular surface and 0.32±0.04 seconds for deep zone, times that are considerably shorter than τ_{PE}, but longer than $\tau_{1,VE}$. Therefore, interstitial fluid did not have enough time to diffuse, resulting in negligible poroelastic energy dissipation, and only a portion of the intrinsic viscoelastic energy dissipation [1,2,6,7]. Thus, loading was likely carried by tension of collagen fibrils induced by pressurized interstitial fluid [1,3,4], and eventually a crack was initiated by breaking covalent bonds between tropocollagen molecules [15,16].

Conversely, at 1 μm/s, the total work likely included energy dissipation from a combination of poroelasticity and viscoelasticity, in addition to the work used to create a crack. Crack nucleation occurred at 390.45±75.54 seconds for articular surface and 618.99±104.95 seconds for deep zone after loading, times that were relatively long compared to all time constants. Thus, both poroelastic and viscoelastic energy dissipation are expected to contribute to the total work [1,2,6,7]. Repulsive forces between proteoglycans may have supported the load [2,5] until a crack was eventually created in tensed collagen fibers by breaking covalent bonds between tropocollagen molecules [15,16].

Depth-dependent fracture behavior can be interpreted based on known spatial variation in structure (i.e., direction, density, and diameter of fibrils [17]) and composition (i.e., proteoglycans distribution and water content [17]). Such variations alter poroelastic and intrinsic viscoelastic characteristics, resulting in different total work required for crack nucleation.

SIGNIFICANCE: Understanding rate-dependent crack nucleation in cartilage provides insight into failure processes that can ultimately lead to osteoarthritis.

REFERENCES: [1] Nia+, *Biophys. J.*, 2011; [2] Nia+, *ACS Nano*, 2015; [3] Li+, *J. Biomech. Eng.*, 2003; [4] Li+, *Med. Eng. Phys.*, 2008; [5] Han+, *Biophys. J.*, 2011; [6] Huang+, *J. Biomech. Eng.*, 2001; [7] Huang+, *J. Biomech. Eng.*, 2003; [8] Broom+, *Arthritis & Rheumatism*, 1990; [9] Simha+, *J. Mater. Sci. Mater. Med.*, 2004; [10] Hu+, *Appl. Phys. Lett.*, 2010; [11] Miller+, *Osteoarthritis Cartilage*, 2010; [12] Desrochers+, *Osteoarthritis Cartilage*, 2012; [13] Setton+, *J. Orthop. Res.*, 1995; [14] Chiravarambath+, *J. Biomech. Eng.*, 2009; [15] Depalle+, *J. Mech. Behav. Biomed. Mater.*, 2015; [16] Tang+, *J. R. Soc. Interface*, 2010; [17] Poole+, *Clin. Orthop.*, 2001.

ACKNOWLEDGEMENT: NSF MRI 1428080. We gratefully acknowledge the help provided by Benjamin Stadnick and Richard Nay at Bruker.